

REPORT DOCUMENTATION PAGE

GPO Approved
OASD No. 0704-0188

2

Public reporting burden for this collection of information is estimated to average 1 hour per response, including the time for reviewing instructions, searching existing data sources, gathering and maintaining the data needed, and completing and reviewing the collection of information. Send comments regarding this burden estimate or any other aspect of this collection of information, including suggestions for reducing this burden, to Washington Headquarters Service, Directorate for Information Operations and Reports, 1215 Jefferson Davis Highway, Suite 1204, Arlington, VA 22202-4302, and to the Office of Management and Budget, Paperwork Reduction Project (0704-0188), Washington, DC 20503.

1. AGENCY USE ONLY (Leave blank)	2. REPORT DATE February 15, 1994	3. REPORT TYPE AND DATES COVERED 01 July 93-31 Dec. 93-SBIRPh1-Final
----------------------------------	-------------------------------------	---

4. TITLE AND SUBTITLE Infrared Detectors Based on Si/SiGe Supperlattices and Silicide/SiGe Schottky Barriers Operating Beyond 12 um	5. FUNDING NUMBERS 3005 SS
--	-------------------------------

6. AUTHOR(S) Dr. Vladimir S. Ban	7. PERFORMING ORGANIZATION NAME(S) AND ADDRESS(ES) PD - LD, Inc. 209 Wall Street, Princeton, NJ 08540 Tel. (609) 924-7979
-------------------------------------	--

8. PERFORMING ORGANIZATION REPORT NUMBER F49620-93-C-0042 AFOSR-TR- 94 0134	9. SPONSORING/MONITORING AGENCY NAME(S) AND ADDRESS(ES) AFOSR 110 Duncan Avenue Suite B 115 Bolling AFB DC 20332-0001
---	--

10. SPONSORING/MONITORING AGENCY REPORT NUMBER 94-10522	11. SUPPLEMENTARY NOTES
--	-------------------------

DTIC ELECTE APR 07 1994 S E D

AD-A277 900

12a. DISTRIBUTION/AVAILABILITY STATEMENT not restricted	Approved for public release; distribution unlimited.
--	--

13. ABSTRACT (Maximum 200 words) Work performed in Phase I of this project clearly established the feasibility of using SiGe detectors in the LWIR region. The most important achievements are: * Both, Schottky barrier and multiquantum well structures based on SiGe alloys and capable of detection in the LWIR region have been grown by the RTCVD epitaxial growth method; * For the first time, the selective epitaxial growth of LWIR SiGe detectors on silicon substrates with CMOS circuitry has been demonstrated, thus showing that monolithically integrated detector-multiplexer structures are feasible; * Schottky barrier detectors with cut-off wavelengths exceeding 10 um have been demonstrated; * Extensive spectral response, cut-off wavelength and dark current measurements for Schottky barrier detectors based on Pt silicide/SiGe alloys with Ge content ranging from 0 to 20% have been carried out and discussed.

14. SUBJECT TERMS Infrared Detectors, SiGe alloys, Schottky Barrier Detectors, Multiquantum wells	15. NUMBER OF PAGES 24
--	---------------------------

16. PRICE CODE	17. SECURITY CLASSIFICATION OF REPORT UNCLASSIFIED
----------------	---

18. SECURITY CLASSIFICATION OF THIS PAGE UNCLASSIFIED	19. SECURITY CLASSIFICATION OF ABSTRACT UNCLASSIFIED
--	---

20. LIMITATION OF ABSTRACT

44-6-045

Table of Contents

A. Scope of Phase I Work	3
1. Detectors based on Silicide/SiGe barriers	
2. Detectors based on $\text{Si}_x\text{Ge}_{1-x}$ /Si multiquantum wells	
B. Work Performed	5
I. Epitaxial growth	5
1. Selective epitaxial growth by Rapid Thermal Chemical Deposition (RTCVD)	
2. Growth of Schottky barrier detector structures	
3. Growth of multiquantum well detector structures	
4. Problems with SiGe epitaxy	
II. Processing	13
1. Processing of Schottky barrier detectors	
III. Testing and Characterization	16
1. Spectral response and cutt-off wavelength of Schottky barrier detectors	
2. Summary of optical and electrical measurement of Schottky barrier detectors	
C. Summary and Conclusions	22
D. Acknowledgments	23
References	24

<input checked="" type="checkbox"/>	<input type="checkbox"/>
<input type="checkbox"/>	<input type="checkbox"/>

Availability Codes	
Dist	Avail and/or Special
A-1	

A. Scope of Phase I Work:

In the Phase I of this work we have clearly established the applicability of silicon-like materials for the detection of long-wave infra-red radiation [LWIR]. Specifically, we investigated the operation of detectors based on $\text{Si}_x\text{Ge}_{1-x}$ alloys, [SiGe in further text], in the 8-12 μm region.

Detectors based on silicon-like materials are highly interesting due to the possibility of monolithic integration with read-out electronics for the production of large size focal plane arrays [FPA]. Such FPA can be produced using the well developed VLSI technology and thus be considerably cheaper and more reliable than the commonly used hybrid arrays.

Two types of detectors were considered:

1. Detectors based on Silicide/SiGe barriers [i.e. SSGD]

Schottky barrier detectors based on Pt silicide/Si have found a wide usage in the 3-5 μm band. Infrared cameras with excellent performance, based on 2-dimensional PtSi/Si arrays as large as 512x512 elements are readily available. They are widely used for civilian and military applications. Even more interesting is the 8-12 μm band, where the radiant emittance of 300 K objects peaks. This band is covered mostly by the HgCdTe (MCT) detectors. Due to the problematic nature of this material, it is difficult to make large MCT arrays. It is thus very exciting to contemplate that silicide/SiGe Schottky barrier detectors could be extended to cover the 8-12 μm band. The development of such materials and detectors was the main purpose of this work. Judging from results obtained so far, this work will almost certainly lead to products useful in a wide variety of thermal imaging applications. We have thus submitted a patent disclosure entitled "High Cut-off Wavelength Infrared Photodetectors" to protect our commercial interests.

Strained $\text{Si}_x\text{Ge}_{1-x}$ on Si has a smaller band-gap than silicon with most of the band offset in the valence band (1). It is expected from the Schottky-Mott model that a silicide/ $\text{Si}_x\text{Ge}_{1-x}$ junction will have a smaller p-type Schottky barrier height than the silicide/Si, therefore a longer cutoff wavelength (2). Table 1 compares Schottky barrier heights and cut-off wavelengths for detectors based on silicide/Si and silicide/SiGe.

Table 1. Schottky barrier heights and cut-off wavelengths

$\text{Pd}_2\text{Si} / \text{Si}$	420 meV	3 μm
$\text{Pd}_2\text{Si} / \text{Si}_{(0.8)}\text{Ge}_{(0.2)}$	269 meV	4.6 μm
PtSi / Si	240 meV	5.1 μm
$\text{PtSi} / \text{Si}_{(0.85)}\text{Ge}_{(0.15)}$	140 meV	8.8 μm

The operation principle of the silicide/ $\text{Si}_x\text{Ge}_{1-x}$ infrared detector (3,4), is the same as that of a conventional silicide/Si Schottky barrier detector (i.e., photo-emission of holes from the silicide to the semiconductor). Several studies found that during the metal- $\text{Si}_x\text{Ge}_{1-x}$ reaction, palladium and platinum preferentially react with Si, causing Ge segregation (5,6). This creates defects which consequently pin the Fermi level (7) near midgap leading to a high Schottky barrier height.

In this work we have employed a thin sacrificial layer of silicon to form silicide with a metal evaporated onto it. In the platinum silicide devices we have made, the sacrificial layer was 40Å, and the metal was 25Å. The deposited metal thicknesses were chosen so that the silicon sacrificial cap layer was all consumed in the silicide formation process. This process ensures a Schottky contact with a pure silicide film (without Ge) and, at the same time, eliminates the Ge segregation at the interface which could cause Fermi level pinning.

2. Detectors based on $\text{Si}_x\text{Ge}_{1-x}$ /Si multiquantum wells [i.e. MQWD].

A multiple quantum well detector structure consists of multiple doped quantum wells (e.g. n-type) sandwiched in between undoped barrier layers. At low temperatures, the barrier between the occupied bound states in the quantum wells and the barriers is sufficiently high so that few carriers have enough thermal energy to escape into the barrier, and hence the whole structure has a very low dark conductivity. The photoexcitation mechanism can be designed to occur in either of two ways. First, one can have optical transitions between the occupied bound states and unoccupied higher level bound states in the quantum well. From these higher states, the carriers can then escape either thermally to the barriers or by tunneling to the next well. This gives rise to a photoconductivity that can be detected. This method has the drawback, however, that it leads to high dark currents because of the thin barriers required for tunneling and/or because of the availability of states in the barriers themselves. The second design approach is to design only a single bound state in the quantum well, which the carriers provided by the doping will occupy in equilibrium. The optical excitation of the carriers is then to an extended superlattice state in the continuum just above the barriers. Since current transport is possible in the extended states, no further intermediate steps are required to lead to photoconductivity, and thicker barriers are possible. This leads to very low dark currents. This method also has the advantage that the oscillator strengths for optical transitions to the extended states are larger than to bound states, resulting in higher quantum efficiency. It should be stressed that since the optical transitions are entirely within states from a single band (e.g. conduction or valence band) and not between bands, whether or not the semiconductor system possesses a direct bandgap is not at all important in these types of detectors. It should also be noted that these detectors have a peak response around the photon energy corresponding to the desired transitions, and then decrease for both higher and lower photon energies. This is different than the Schottky barrier detectors, whose response typically increases monotonically at shorter wavelengths. This peaked response at low wavelengths may be helpful in system applications when one is searching for a relatively cold object.

B. Work Performed

Fully operational SSGD detectors operating in the LWIR range have been successfully made and tested. MWQ structures have been grown and characterized. These results will be fully discussed in the ensuing sections.

This work was done in cooperation with Professor J.C. Sturm from the Princeton University, where epitaxial growth and processing of detectors was carried out. Dr. Jimenez from the Rome Laboratories, Hanscom AFB and Mr. Grubisic from EG&G Judson cooperated in testing of detectors.

I. Epitaxial Growth

1. Selective epitaxial growth by Rapid Thermal Chemical Vapor Deposition (RTCVD)

Epitaxial layers of SiGe alloys were grown at Princeton University in a reactor specifically designed for this purpose. The reactor and its mode of operation have been described in several publications by Professor J. Sturm et al.(8,9), so we shall reiterate its main features only briefly.

Figure 1 represents the schematic drawing of the reactor. The growth chamber is a cylindrical quartz tube, which can be pumped to provide conditions for epitaxial growth at reduced pressures. A quick switching inlet valve manifold regulates flow of reactants, (dichlorosilane and germane), and of carrier gas (hydrogen) into the reactor. Diborane and phosphine are used as p and n dopants, respectively.

The wafer is suspended in the growth chamber by several quartz pins, (no susceptor), and heated from one side by a battery of twelve 6 kW tungsten-halogen lamps. This system has a very low thermal mass and the temperature of the wafer can be changed rapidly to optimize the growth temperature. This feature can be exploited in the growth of thin layers in the SiGe/Si system. Silicon can be grown at 700-1000 C and SiGe alloys at 625-700 C, i. e., at respective optimal growth temperatures for both materials.

The Schottky barrier SiGe detectors previously demonstrated by Prof. Sturm's group (3,4), were made from wafers where Si/SiGe layers were grown over the whole area of the substrate wafer. The detector areas were subsequently defined by opening the oxide and forming the Pt or Pd silicides on the underlying Si/SiGe layers.

In this work we have taken the SiGe detector technology an important step further by growing SiGe epitaxial layers selectively on wafers on which the CMOS circuitry has been already processed and then protected by a cover oxide layer. In Phase II this technology will allow us to grow detector structures immediately adjacent to the signal processing circuitry. In the last processing step, the appropriate areas can be opened to deposit metallization pattern which provides contacts to and between detectors and CMOS devices on the wafer.

We have thus demonstrated a technology capable of producing fully integrated LWIR FPAs based on silicon and silicon-like materials.

2. Growth of Schottky barrier detector structures

The epitaxial structure for SSGDs is schematically shown in Figure 2. Typically, it consists of silicon buffer layers, linearly graded SiGe layers, a constant composition SiGe layer and a silicon cap layer. The function of graded layers is to accommodate lattice mismatch between the silicon substrate and the final SiGe layer with constant composition, which is the light absorption layer. This layer may contain as much as 20% Ge. Silicon cap layer is designed to be consumed in the silicide formation reaction.

Silicon buffer layers were grown at 1000 C; the first layer was 1 μm thick, p+ doped with boron, and the second silicon layer was 1.5 μm thick, grown unintentionally doped, but doped to p- by autodoping. These substrates were then used to fabricate detectors by growing SiGe layers and the silicon cap layer.

In the accompanying Table II we list conditions for the growth of 4 epitaxial structures, consisting of layers described above. In all growth runs the flow of hydrogen was 3000sccm, the reactor pressure was 6 torr and the growth temperatures are indicated in the table.

Samples #1329, #1330, #1331 and #1332 were designed to have cut-off wavelengths of 10, 9, 7.5 and 6 μm , respectively. The respective percentages of germanium in the absorption SiGe layers were 20, 14, 11 and 7%.

For illustrative purposes we shall briefly discuss the growth of sample # 1329. As mentioned previously, the substrate is a silicon wafer with buffer layers already grown. The growth of SiGe epitaxial structures commences by depositing a thin layer of silicon; the growth temperature is 700 C, pressure is 6 Torr, dichlorosilane flow is 26 sccm and hydrogen flow is 3000 sccm. After 1 minute one initiates flow of germane[0.8% GeH_4 in hydrogen], gradually increasing it to a flow of 50 sccm, over 225 seconds. This brings Ge content to 13%; the approximate thickness of the SiGe layer is 100 A. Then the next grading layer is grown by increasing germane flow from 50 to 100 sccm over 120 seconds. The thickness of this layer is about 150 A and the final Ge content is nominally 20%. One then proceeds to grow the final SiGe layer, at germane flow of 100 sccm and dichlorosilane flow of 26 sccm over 180 seconds to a thickness of 300 A and with a nominal composition of 20% Ge. Lastly, the silicon cap is grown for 80 seconds to a thickness of 40 A. The wafer is now ready for processing into a detector.

3. Growth of multi-quantum well detector structures

A peak response at normal incidence of 8 μm was obtained for $\text{Si}_{0.85}\text{Ge}_{0.15}$ multi-quantum wells (10). The 8 μm peak corresponds to a transition energy of 150 meV . In order to achieve a 12 μm peak response [energy of 100 meV], one should reduce the Ge concentration to about 10% and/or reduce well thickness.

We used RTCVD reactor to grow a MQW epitaxial structure shown in Figure 3. The substrate is a (100) p-type silicon wafer on which a 0.1 μm thick, p+ boron doped contact layer is grown. This is followed by the growth of 15 periods of multiple quantum wells, consisting of 300A thick silicon barrier layers and 40A thick $\text{Si}_x\text{Ge}_{1-x}$ layers, where Ge content is 12-14%. Difficulties with controlling the composition of epitaxial SiGe layers

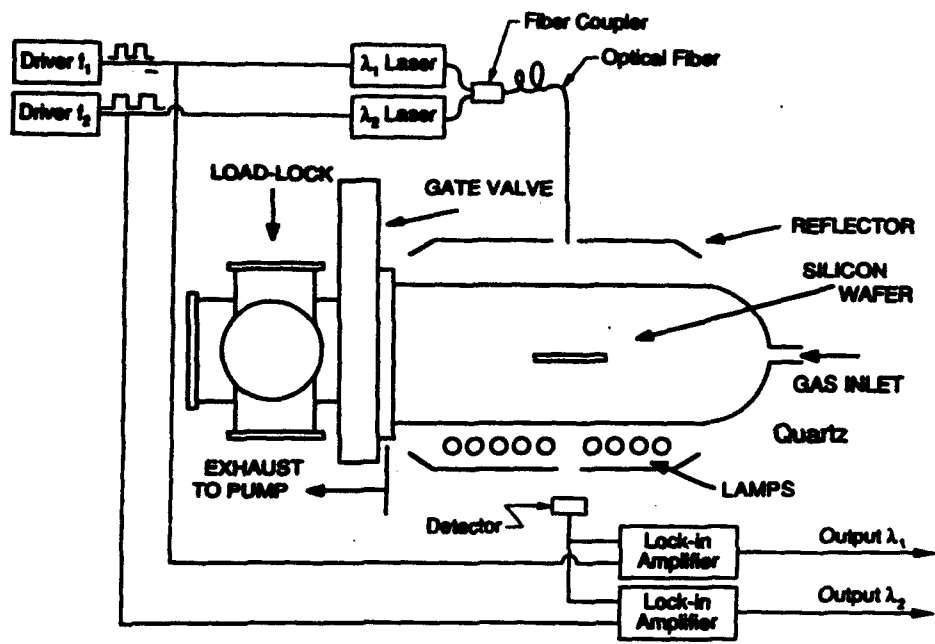


Figure 1. Schematic representation of RTCVD reactor

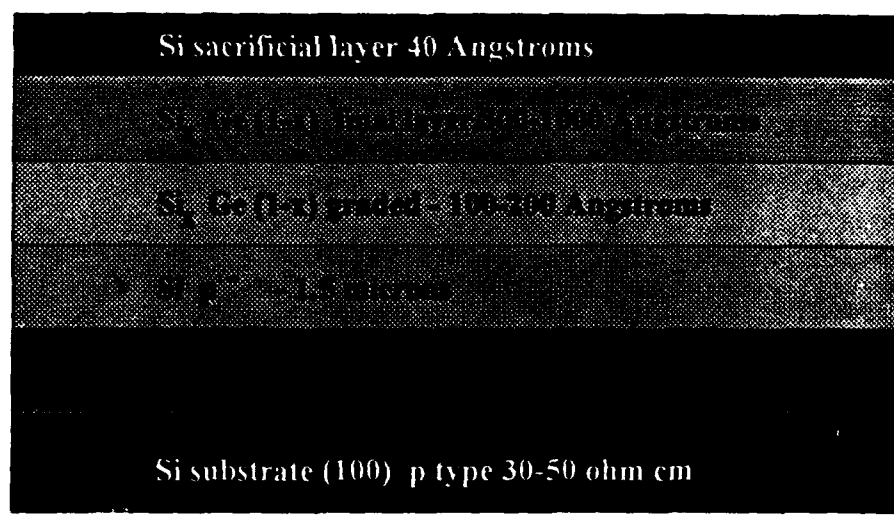


Figure 2. Epitaxial structure for the Schottky barrier detector

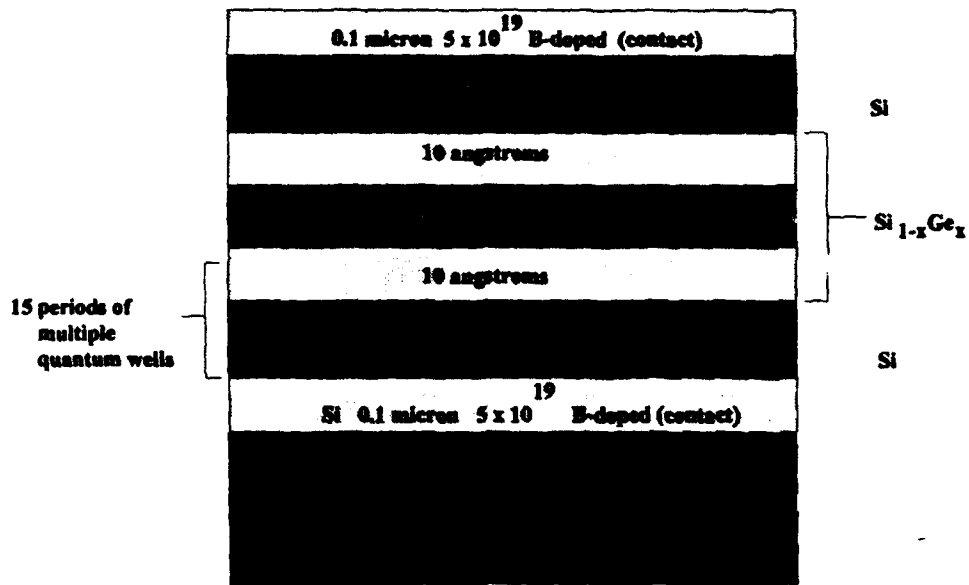


Figure 3. Epitaxial structure for the multiquantum well Si/SiGe detectors

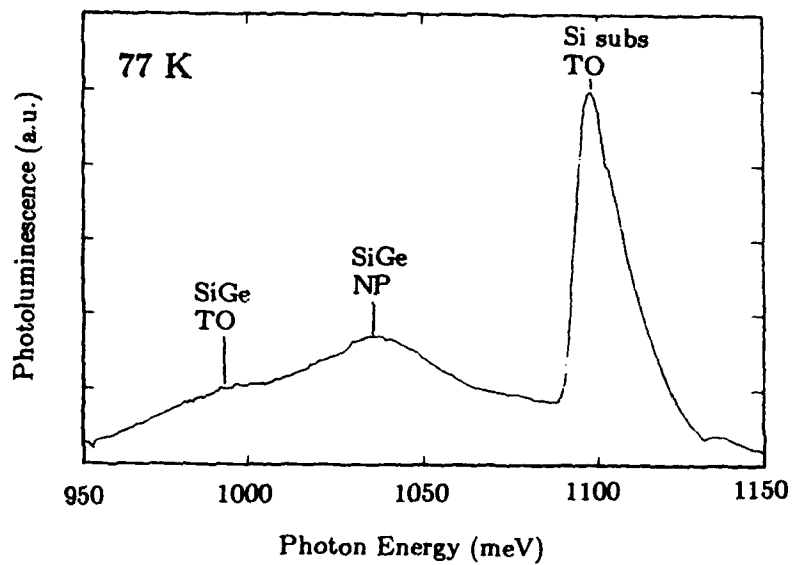


Figure 4. Photoluminescence spectra of Si/SiGe multiquantum well structure

are discussed in the next section. The outer 10A of these layers are intrinsic, while the inner 20A are p+ doped [boron].

Figure 4 shows photoluminescence spectra of grown layers taken at 77 K. The difference between the TO transition for silicon, (~ 1090 meV), and TO transition for SiGe layers, (~ 990 meV), corresponds to the energy difference required for the LWIR detection (~ 100 meV).

Figures 5 and 6 show TEM micrographs of Si/SiGe multiquantum wells grown in the RTCVD reactor, at magnifications of 375,000 X and 1,950,000 X, respectively. Note that structures at nm scale can be grown (SiGe layers appear dark).

4. Problems with SiGe epitaxy

There are several potential problems with the control of the composition, thickness and uniformity of epitaxial layers of SiGe alloys.

a. Non-linear relation between the growth rate of SiGe alloys and the flow of germane: Figure 7a shows that the growth rate of SiGe alloys decreases in a non-linear fashion with the increasing flow of GeH_4 . This makes a control of thickness of grown layers difficult.

b. Non-linear relation between the Ge content in the epitaxial layers and the flow of GeH_4 . Figure 7b shows that the content of Ge does not increase linearly with the flow of germane; this makes the control of the composition of SiGe epitaxial layers difficult. Figure 7c shows that there can be significant deviations between the desired and the actual thickness and composition of the grown layers. This has important practical implications, because the composition of epitaxial layers determines the cut-off wavelength of the detector, while the thickness controls effects of the lattice mismatch, which influence the level of the dark current and thus the noise performance of detectors.

c. Thickness and composition non-uniformities over the wafer

Since the wafers in the RTCVD reactor are directly heated by the radiation lamps, there might be some temperature non-uniformity across the wafer, which can lead to the spatial non-uniformity in thickness and composition. This might pose a problem for the LWIR detectors, which require highly uniform wafers to read small temperature differences in infrared images.

In Phase II we plan to address and eliminate problems with epitaxial growth of SiGe layers listed above. Issues of the thickness and compositional control will be solved by a series of careful calibration runs, designed to elucidate the exact relation between the flow of germane and these variables. The spatial non-uniformities can be solved by the introduction of a susceptor, which will reduce spatial thermal differences. With these improvements it is reasonable to assume that high quality wafers, suitable for the production of LWIR FPAs can be made.

Table II

GROWTH OF SiGe/Si EPITAXIAL LAYERS WITH 7, 11, 14 AND 20% Ge

		Sample 1329	Sample 1330	Sample 1331	Sample 1332
Expected cut off	um	10	9	7.5	6
Grading 1					
Duration	sec	225	225	120	120
Thickness	A	100	100	150	150
Composition	%Ge	0 to 13	0 to 13	0 to 7	0 to 7
Growth temp.	C	625	625	700	700
Grading 2					
Duration	sec	120	na	60	na
Thickness	A	150	na	250	na
Composition	%Ge	13 to 20	na	7 to 11	na
Growth temp.	C	625	na	700	na
Final SiGe layer					
Duration	sec	180	720	120	360
Thickness	A	300	650	600	1200
Composition	%Ge	20	14	11	7
Growth temp.	C	625	625	700	700
Si Cap					
Duration	sec	80	80	80	80
Thickness	A	40	40	40	40
Growth temp.	C	700	700	700	700

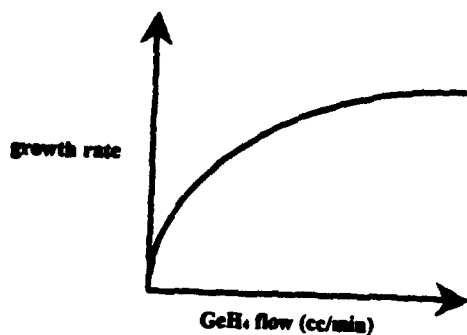


Figure 5. TEM micrograph of Si/SiGe MQW (x=375 K)

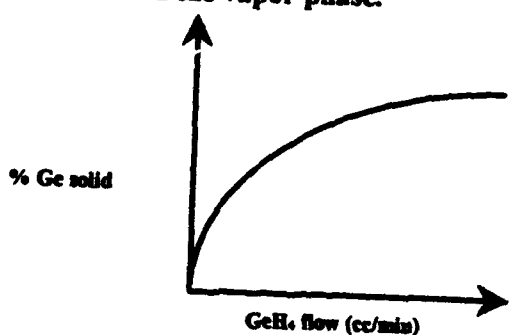


Figure 6. TEM micrograph of Si/SiGe MQW (x=1950 K)

1. Non linear relation between the growth rate of SiGe alloys and the flow of GeH₄



2. Non-linear relation between the Ge content in the solid and the GeH₄ concentration in the vapor phase.



3. Due to the above non-linearities, it is difficult to control the thickness and composition of SiGe epitaxial layers.

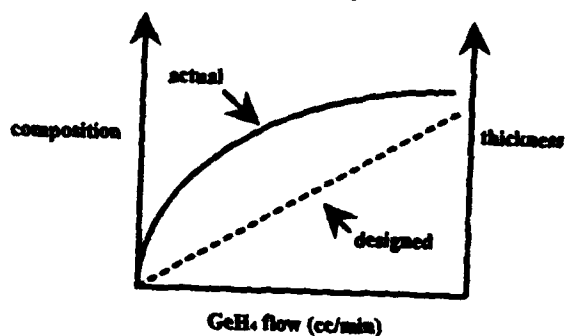


Figure 7. Potential problems with epitaxial deposition of Si/SiGe structures

II. Processing

1. Processing of Schottky barrier detectors

Schottky barrier detectors based on SiGe alloys have been recently demonstrated in Prof. Sturm's group at Princeton University (3,4). In difference with the previously demonstrated detectors, devices produced under this contract are based on SiGe layers grown by the selective epitaxy on Si wafer. This approach yields devices, which can be readily integrated with the CMOS circuitry already processed on that wafer. The production of fully integrated, silicon based detectors and multiplexers is the main long term objective of our work.

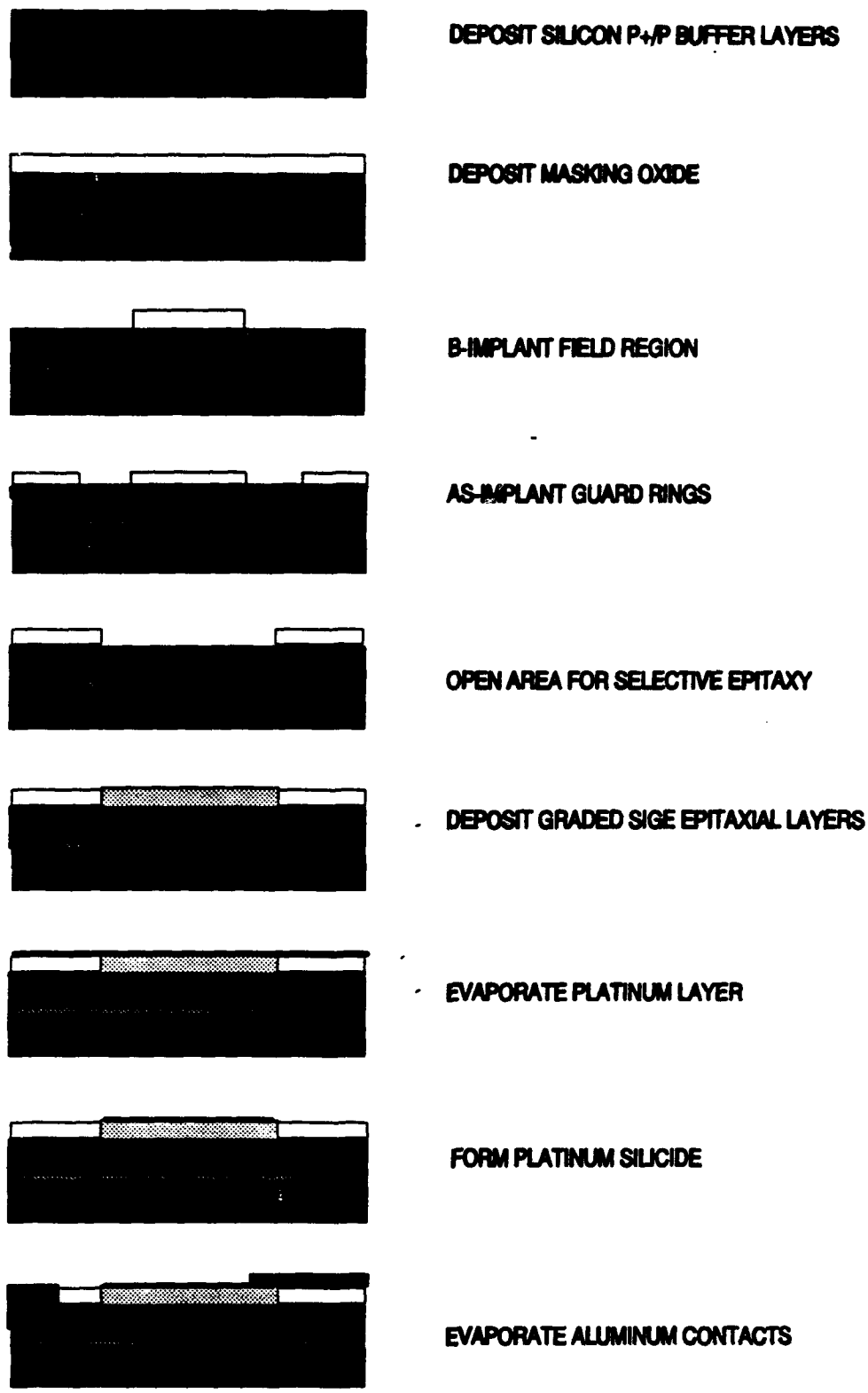
The selective epitaxy of SiGe alloys is a novel process, and our first task was to design a processing sequence for detectors based on the selectively grown areas. The following is the preliminary processing sequence for these devices:

Substrate: Silicon, p-type 30-50 ohm-cm, orientation (100)

- Step 1: Epitaxially grow 1um silicon, p-type, boron doped $3 \times 10^{19} / \text{cm}^3$
- Step 2: Epitaxially grow 1.5 um silicon, undoped, (p-)
- Step 3: Deposit 0.5 um masking oxide (plasma)
- Step 4: Litho 1-etch alignment marks
- Step 5: Litho 2- open holes in oxide
- Step 6: Implantation 1- B implant field region
- Step 7: Strip and redeposit oxide
- Step 8: Litho 3- open guard rings in oxide
- Step 9: Implantation 2- As implant guard rings
- Step 10: Strip all oxide
- Step 11: Grow final field oxide-2200 A, 1000 C , sequence dry/wet/dry oxide
- Step 12: Litho 4-open areas for selective epitaxy of SiGe layers
- Step 13: Grow selective epitaxial layers of $\text{Si}(x)\text{Ge}(1-x)$, where x determines cut-off
- Step 14: Evaporate 30 A of platinum
- Step 15: Anneal at 300-400 C to form Pt-silicide on selectively grown areas
- Step 16: Etch unreacted platinum
- Step 17: Litho 5- define areas for substrate p+ contacts
- Step 18: Etch field oxide (wet) and silicon (plasma) to reach p-region
- Step 19: Litho 6- define metallization pattern
- Step 20: Evaporate 5000 A of aluminum on the front side
- Step 21: Lift-off aluminum and remove photoresist
- Step 22: Evaporate aluminum on the back side
- Step 23: Anneal contacts- 20 min. at 400 C in forming gas

Figure 8 schematically shows the processing sequence for the production of Pt silicide/SiGe Schottky barrier detectors.

Figure 9 schematically shows the LWIR Schottky barrier detector produced by the above processing sequence.



DEPOSIT SILICON P+/P BUFFER LAYERS

DEPOSIT MASKING OXIDE

B-IMPLANT FIELD REGION

AS-IMPLANT GUARD RINGS

OPEN AREA FOR SELECTIVE EPITAXY

DEPOSIT GRADED SIGE EPITAXIAL LAYERS

EVAPORATE PLATINUM LAYER

FORM PLATINUM SILICIDE

EVAPORATE ALUMINUM CONTACTS

Figure 8. Processing sequence for Schottky barrier detectors grown by selective epitaxy

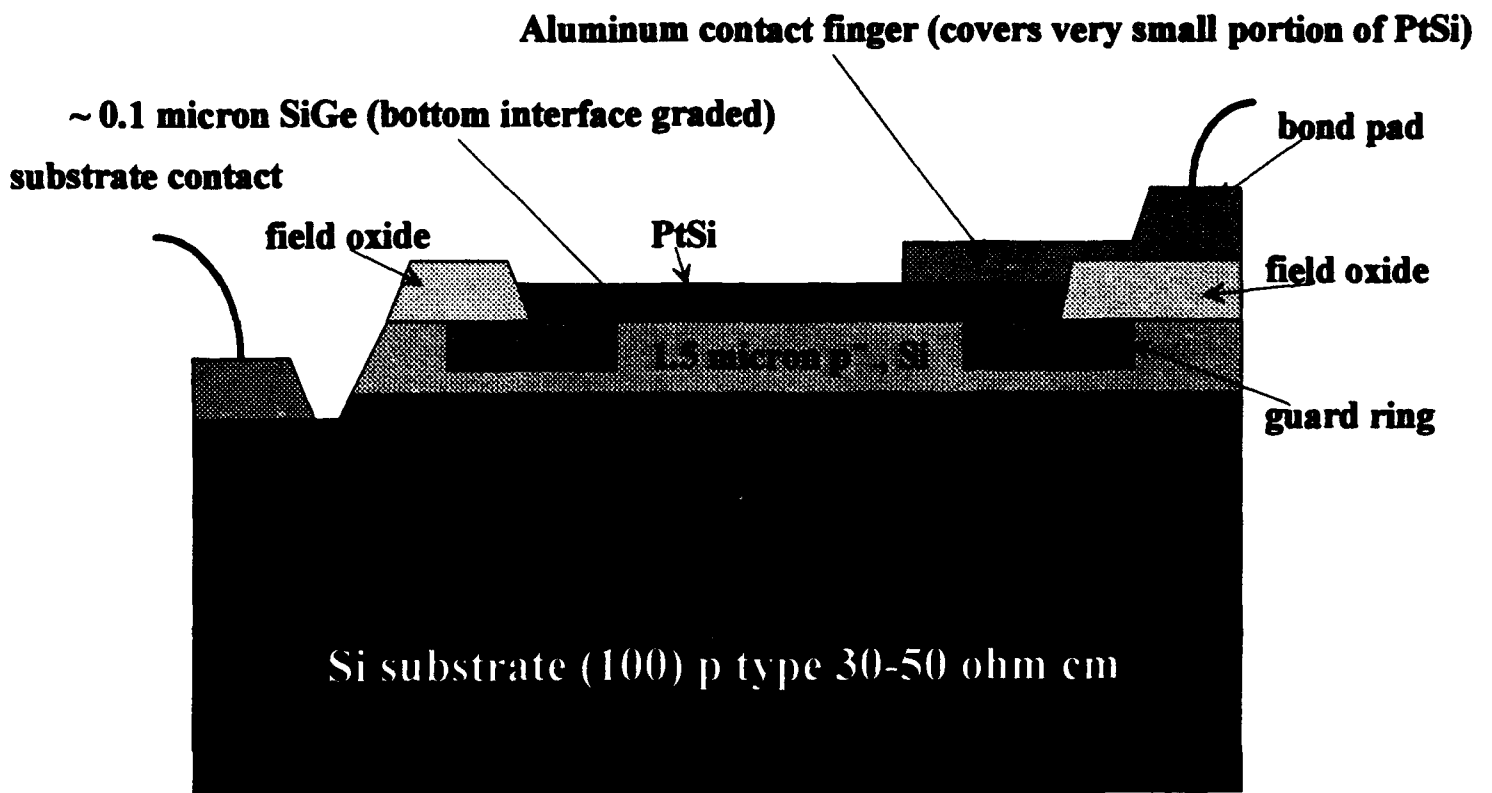


Figure 9. Schematic representation of a Schottky barrier detector

III. Testing and Characterization

1. Spectral response and cut-off wavelength of Schottky barrier detectors

a. Fowler plots

The photoresponse of Schottky barrier detectors results from the injection of photoexcited hot holes from the silicide film into the silicon substrate. Figure 10 shows the schematic band diagram of a Schottky barrier detector. Holes must gain enough energy from the incoming photons to be able to surmount the barrier at the interface, which means that the photon energy must be larger than the Schottky barrier height. The Schottky barrier, ϕ_b , thus determines the cut-off wavelength, λ_c , via the equation:

$$\lambda_c = 1.24/\phi_b \quad (1)$$

Thus, to obtain cut-off wavelength of 10 μm , the Schottky barrier height must be less than 0.124 eV.

The spectral response of a Schottky barrier detector is given by a Fowler equation, which shows that the external quantum efficiency, Y , is a function of the photon energy, $h\nu$:

$$(Yh\nu)^{0.5} = C^{0.5}(h\nu - \phi_b) \quad (2)$$

C is the so called quantum efficiency constant determined by the properties of a given silicide material.

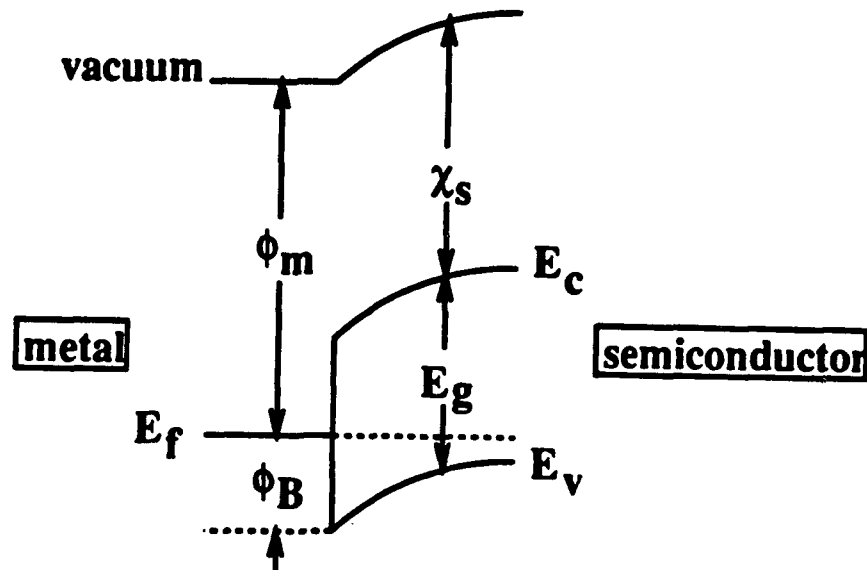


Figure 10. Schottky barrier to a p-type semiconductor.

Thus the plot of the square root of the quantum efficiency Y versus the photon energy $h\nu$ should be a straight line. By linearly extrapolating to zero response one can find value of the Schottky barrier ϕ_b ; the slope of the line equals to the square root of C .

Figures 11a and 11b show Fowler plots of two Schottky barrier detectors based on Pt silicide/ $\text{Si}_{0.8}\text{Ge}_{0.2}$ structures, measured at 20 K and 2V reverse bias. The results show that $\lambda_c > 10 \mu\text{m}$ has been achieved.

A very interesting discovery has been made that the cut-off wavelength depends on the reverse bias of the detector. This is shown in the Figure 12, where λ_c varies from 4 μm at 0V to 10 μm at -2.2V. This means that these detectors have an inherent spectral filter which can be activated by the bias applied to the device! This phenomenon can be explored in the Phase II of this program.

b. Dark current measurements

Another method of determining the barrier potential of a Schottky barrier detector is to measure the dark current of the device. Dark currents in detectors have several sources: thermionic emission, carrier diffusion, recombination currents and tunnelling. From thermionic emission theory, which assumes that the thermionic hole emission is the main source of the dark current, one can describe the I-V characteristics of the diode by the following equation:

$$J = A^* T^2 e^{-q\phi_{el}/kT} (e^{qV/kT} - 1) \quad (3)$$

where: J =current density; A^* =Richardson constant; ϕ_{el} =potential barrier to thermally generated carriers, which is close but not identical to the ϕ_b ; q =electron charge; V =applied bias; T =absolute temperature.

Figures 13a and 13b show the reverse and forward I-V characteristics of detector with 20% Ge.

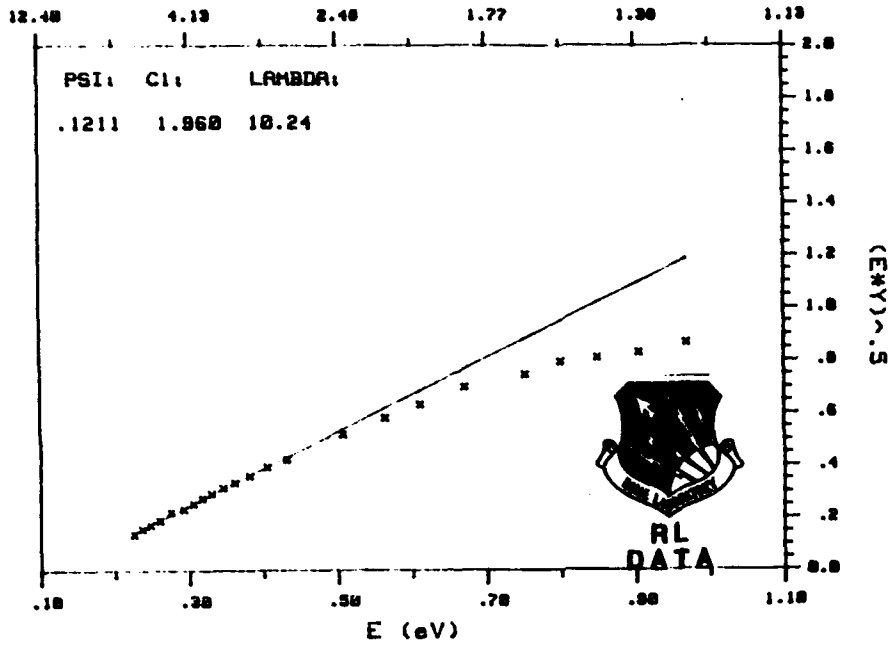
Figure 14 shows the plot of J/T^2 versus $1/T$, from which values of the electrical barrier ϕ_{el} and of the Richardson constant can be determined.

3. Summary of optical and electrical measurements of Schottky barrier detectors

Table III summarizes results obtained for the 2 groups of Schottky barrier detectors with a nominal germanium content of 0, 5, 10, 15 and 20%, respectively. This table lists values of Ψ_{opt} which is equivalent to ϕ_b , of Ψ_{elect} which is equivalent to ϕ_{el} , as well as values of C and A^* for these devices. Furthermore, I-V data are also listed.

The above measurements were done through a courtesy of Dr. J. Jimenez from the Rome Laboratory, Hanscom AFB.

SCHOTTKY ELECTRO-OPTICAL PARAMETERS
 DEVICE: STRMG_9_4 METAL: Pt
 DATE: 8 Nov 1993 THICKNESS:
 COMMENTS: 20%Ge/FORMG GAS



SCHOTTKY ELECTRO-OPTICAL PARAMETERS
 DEVICE: STRMG_9_3 METAL: Pt
 DATE: 8 Nov 1993 THICKNESS:
 COMMENTS: 20%Ge/FORMG GAS

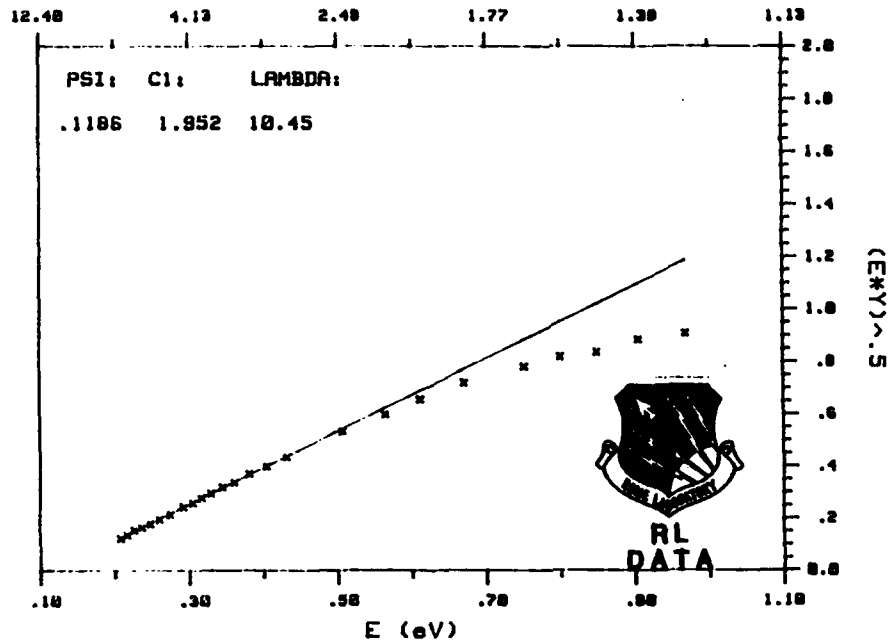


Figure 11. Fowler plots for detectors with 20% Ge showing cut-off wavelengths exceeding 10 um

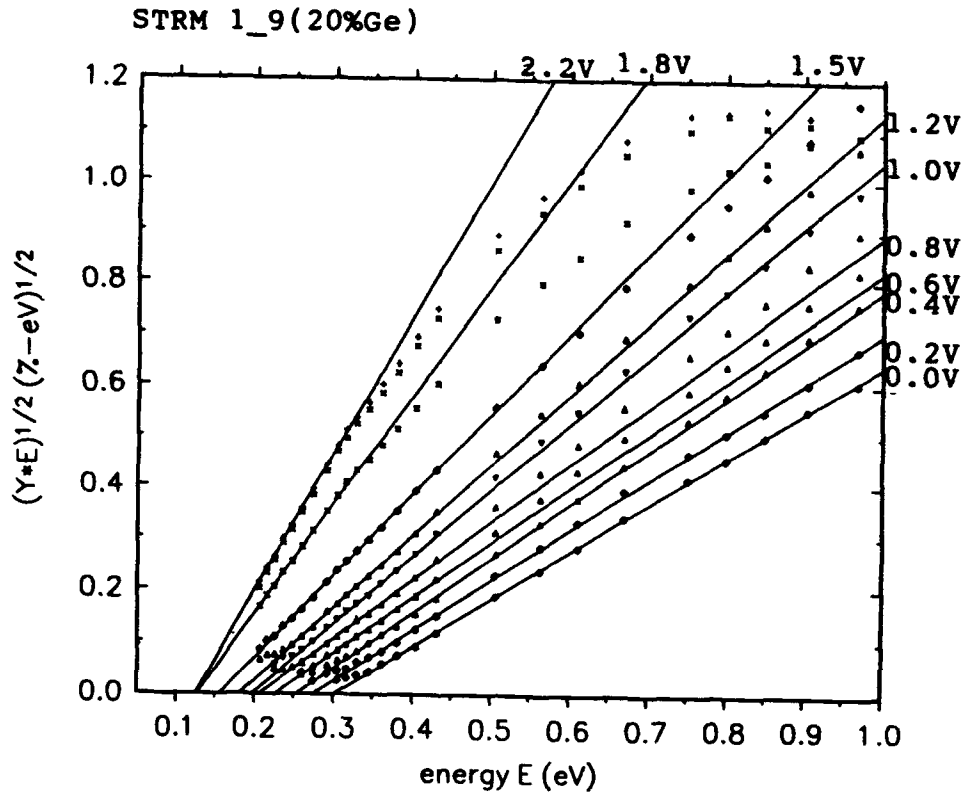


Figure 12. Dependence of cut-off wavelength on reverse bias

STRM6_9 (PtSi) T = 20, 30, 40, 60, 77 K 15NOV93

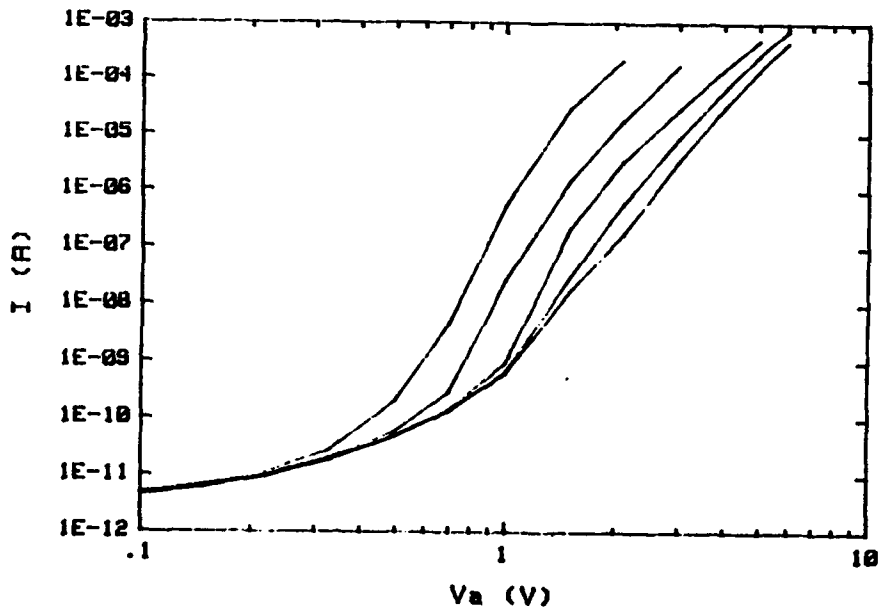


Figure 13a. Reverse I-V characteristics of 20% Ge detector

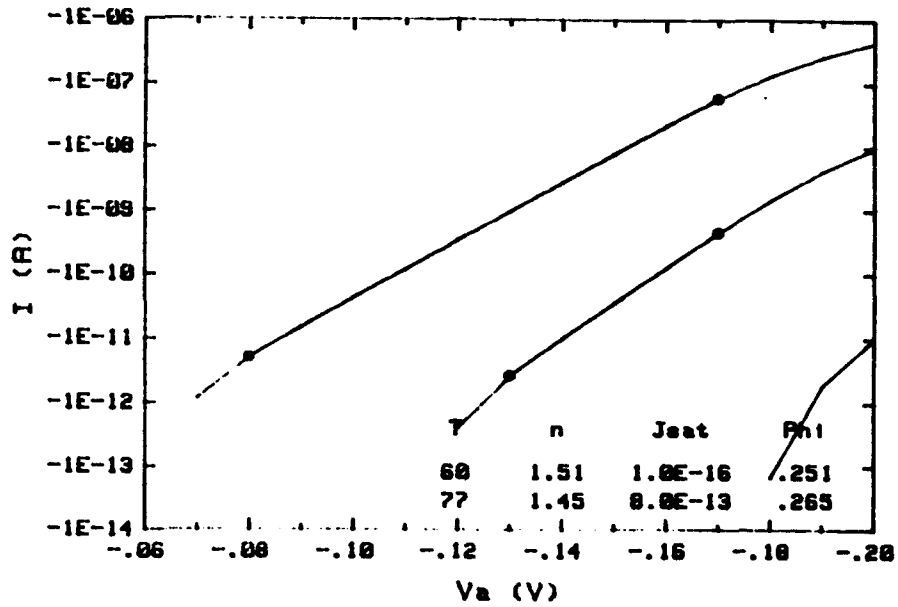


Figure 13b. Forward I-V characteristics of 20% Ge detector

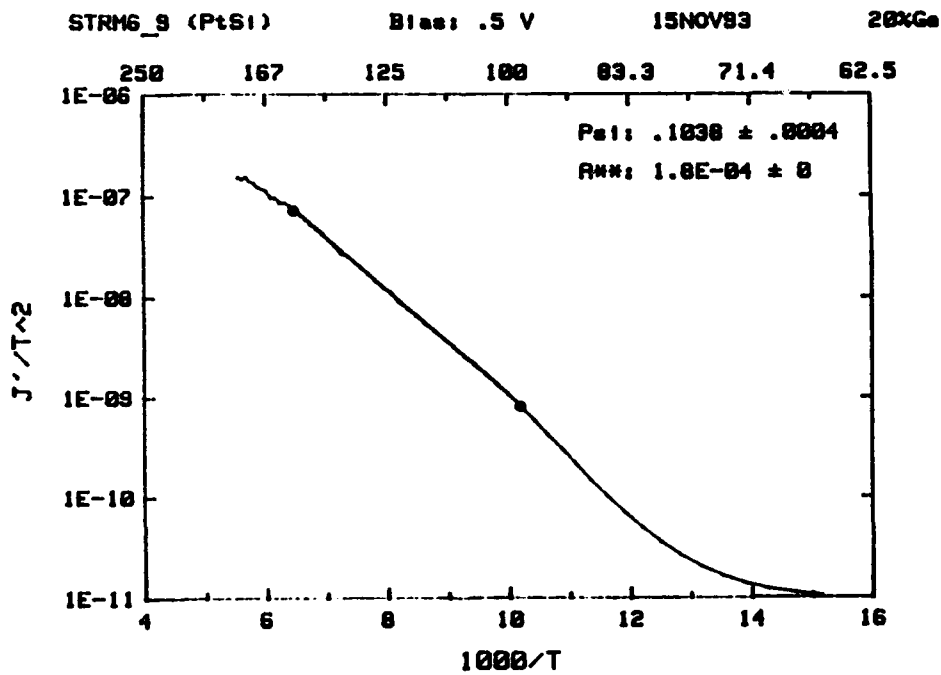


Figure 14. Barrier potential by dark current measurement

Table III. Summary of electrical and optical measurements of 2 groups of Schottky barrier detectors with Ge content from 0 to 20%

ID	Info	Yield		Dark Current		Reverse I-V's		
		ψ_{opt} (eV)	C_s (%/eV)	ψ_{dark} (eV)	A^{**}	Brkdown(V)	Noise Fir(I)	60K, @10V
STRM 1	20% Ge	0.128	6.9	0.115	0.1	0.6	8×10^{-12}	4×10^{-10}
STRM 2	15% Ge	0.155	12.3	0.069	0.1	0.5	1×10^{-11}	1×10^{-9}
STRM 3	10% Ge	0.172	9.9	0.112	0.9	linear	1×10^{-13}	4×10^{-10}
STRM 4	5% Ge	0.180	9.9	0.149	5.3	linear	2×10^{-13}	2×10^{-10}
STRM 5	0% Ge	0.208	18.7	0.158	2.1	0.6	1×10^{-9}	1×10^{-9}
STRM 6	20% Ge	0.139	1.7	---	---	0.5	7×10^{-12}	8×10^{-10}
STRM 7	15% Ge	0.158	15.3	0.079	0.2	0.2	4×10^{-12}	1×10^{-9}
STRM 8	10% Ge	0.173	12.9	0.178	0.6	linear	1×10^{-13}	1×10^{-9}
STRM 9	5% Ge	0.187	10.7	0.189	2.1	0.2	3×10^{-13}	5×10^{-10}
STRM 10	0% Ge	0.215	19.3	0.187	9.8	2.2	1.5×10^{-9}	2×10^{-9}

23Nov93, MMW

Yield data at $V_{opt} = 2.0V$.

Dark Current data at $V_{dark} = 2.0V$, except for STRM 1, 9, and 10 which were at 1.0V, and STRM 8 which was at 0.5V

C. Summary and Conclusions

Work performed in Phase I of this project clearly established the feasibility of using SiGe detectors in the LWIR region. The most important achievements are:

1. Both, Schottky barrier and multiquantum well structures based on SiGe alloys and capable of detection in the LWIR region have been grown by the RTCVD epitaxial growth method;
2. For the first time, the selective epitaxial growth of LWIR SiGe detectors on silicon substrates with CMOS circuitry has been demonstrated, thus showing that monolithically integrated detector-multiplexer structures are feasible;
3. Processing sequence for the selectively grown, guard ring protected Schottky barrier detectors has been developed and successfully applied to produce a series of detectors with Ge content ranging from 0 to 20%;
4. Schottky barrier detectors with cut-off wavelengths exceeding 10 μm have been demonstrated;
5. SiGe/Si multiquantum well structures have been characterized by means of TEM and photoluminescence;
6. Extensive spectral response, cut-off wavelength and dark current measurements for Schottky barrier detectors based on Pt silicide/SiGe alloys with Ge content ranging from 0 to 20 % have been carried out and discussed.

D. Future Work

In the Phase II proposal we describe in detail our plans to develop and produce fully integrated LWIR FPAs based on Pt silicide/ SiGe alloy Schottky barrier detectors. In this effort we shall closely cooperate with Professors J. Sturm's group at Princeton University and Dr. G. Hughes' group at the David Sarnoff Research Center in Princeton (DSRC).

Main tasks in Phase II are:

1. Increase our understanding of epitaxial processes in order to improve thickness and compositional uniformity of epitaxial layers of SiGe;
2. Selectively grow SiGe detector structures on multiplexer wafers supplied by the DSRC and thus demonstrate the monolithically integrated LWIR FPA based on VLSI technology;

3. Fully characterize the SiGe FPA at the DSRC Infrared Measurement Laboratory to assess its applicability to LWIR imaging.

E. Acknowledgments

PD-LD, Inc. gratefully acknowledges the Air Force Office of Scientific Research Phase I SBIR grant for this work (contract # F49620-93-C-0042).

We are also grateful to Prof. J. Sturm, Princeton University, Dr J. Jimenez, Rome Laboratories, Hanscom AFB and Mr D. Grubisic, EG&G, Judson for their many contributions to the success of this work.

References:

1. C.G. Van de Walle and R.M. Martin, *Phys. Rev. B*, 34, 5621 (1986)
2. H. Kanaya, F. Hasegawa, E. Yamaka, T. Moriyama, and M. Nakajima, *Japan.J. Appl. Phys.* 28, L544 (1989)
3. X Xiao, Ph.D. Thesis, Princeton University 1993
4. X.Xiao, J.C. Sturm, S.R. Parihar, S.A. Lyon, D. Meyerhofer and S. Palfrey, *IEDM 92, Tech. Digest* p. 125 (1992)
5. H. Kanaya, Y. Cho, F. Hasegawa, and E. Yamaka, *Japan. J. Appl. Phys.* 29, L850 (1991)
6. H.K. Liou, X. Wu, U. Gennser, V.P. Kesan, S.S. Iyer, K.N. Tu, and E.S. Yang, *Appl. Phys. Lett.*, 60, 577 (1992)
7. C.M. Gronet, J.C. Sturm, K.E. Williams, J.F. Gibbons, and S.D. Wilson, *Appl.Phys. Lett.* 48, 1012 (1986)
8. J.C. Sturm, P.V. Schwartz, E.J. Prinz, and H. Manoharan, *J. Vac. Sci. Tech.*,B9, 2011 (1991)
9. J.C. Sturm, P.M. Garone and P.V. Schwartz, *J.Appl. Phys.*, 69, 542 (1991)
10. J.S. Park, R.P.G. Karunasiri and K.ZL. Wand, *Appl. Phys. Lett.* 60, 103 (1992).